

Article

A New Golden Eagle Optimization with Stooping Behaviour for Photovoltaic Maximum Power Tracking under Partial Shading

Zhi-Kai Fan ¹, Kuo-Lung Lian ^{1,*} and Jia-Fu Lin ²

¹ Department of Electrical Engineering, National Taiwan University of Science and Technology, No. 43, Section 4, Keelung Rd., Taipei City 106, Taiwan; d11107012@gapps.ntust.edu.tw

² Taiwan Power Company, No. 242, Section 3, Roosevelt Rd., Zhongzheng District, Taipei City 100208, Taiwan; m10907108@mail.ntust.edu.tw

* Correspondence: ryanlian@gapps.ntust.edu.tw

Abstract: Solar photovoltaic (PV) systems often encounter a problem called partial shading condition (PSC), which causes a significant decrease in the system's output power. To address this issue, meta-heuristic algorithms (MHAs) can be used to perform maximum power point tracking (MPPT) on the system's multiple-peak P-V curves due to PSCs. Particle swarm optimization was one of the first MHA methods to be implemented for MPPT. However, PSO has some drawbacks, including long settling time and sustained PV output power oscillations during tracking. Hence, some improved MHA methods have been proposed. One approach is to combine a MHA with a deterministic approach (DA) such as P & O method. However, such a hybrid method is more complex to implement. Also, the transition criteria from a DA to a MHA and vice versa is sometimes difficult to define. Another approach, as adapted in this paper is to modify the existing MHAs. This includes modifying the search operators or the parameter settings, to enhance exploration or exploitation capabilities of MHAs. This paper proposed to incorporate the stooping behaviour in the golden eagle optimization (GEO) algorithm. Stooping is in fact a hunting technique frequently employed by golden eagles. Inclusion of stooping in the GEO algorithm not only truly model golden eagles' hunting behaviour but also yields great performance. Stooping behavior only requires one extra parameter. Nevertheless, on average, the proposed method can reduce tracking time by 42.41% and improve dynamic tracking accuracy by 1.95%, compared to GEO. Moreover, compared to PSO, GWO, and BA, the proposed method achieves an improvement of 2.66%, 3.56%, and 4.24% in dynamic tracking accuracy, respectively.

Keywords: partial shading condition; maximum power point tracking; photovoltaic system; golden eagle optimizer



Citation: Fan, Z.-K.; Lian, K.-L.; Lin, J.-F. A New Golden Eagle Optimization with Stooping Behaviour for Photovoltaic Maximum Power Tracking under Partial Shading. *Energies* **2023**, *16*, 5712. <https://doi.org/10.3390/en16155712>

Academic Editors: Doug Arent, Adam Warren and Xiaolei Yang

Received: 28 June 2023
Revised: 23 July 2023
Accepted: 29 July 2023
Published: 31 July 2023



Copyright: © 2023 by the authors. Licensee MDPI, Basel, Switzerland. This article is an open access article distributed under the terms and conditions of the Creative Commons Attribution (CC BY) license (<https://creativecommons.org/licenses/by/4.0/>).

1. Introduction

Solar energy is one of the most promising sources of renewable energy and its global installation is expected to hit 1870 GW by 2025. One of the biggest issues with PV systems is partial shading. Typically, this is due to tall structures, clouds, trees, snow, and dust on neighbouring PV modules. Shaded modules provide less power than unshaded modules in partial shading conditions (PSCs). The shaded modules place a limit on the output power and may result in uneven current flow. Localized hotspots are resulted due to the mismatch losses in the PV arrays. To overcome the hotspot problem, each module is installed with a bypass diode. Nevertheless, this results in multiple peaks in power-voltage or power-current curves.

Attaining the global maximum power point (GMPP) of a P-V curve is essential for generating the maximum power. Up to 70% of the output power of a PV system may be lost if a maximum power point tracking (MPPT) system is unable to find the GMPP [1]. There are two different ways to alleviate PSC issues to prevent this—hardware and software approaches.

Reconfiguring the hardware is the first way. The electrical array reconfiguration (EAR) technique is applied to the PV array to reduce mismatch loss under PSCs. The hardware approach reconfigures the electrical connections of solar PV panels to mitigate shading effects. Nevertheless, the necessity for numerous switches, sensors, and control algorithms makes large-scale deployment challenging.

Software solutions for maximum power point tracking (MPPT) under PSCs focus on developing advanced algorithms without requiring additional hardware, making them cost-effective. There are mainly three types of software solutions: deterministic approaches (DAs), meta-heuristic approaches (MHAs) and artificial intelligence (AI) methods.

Deterministic approaches such as perturb-and-observe (P & O) [2,3], hill climbing [4], and incremental conductance [5] essentially employ greedy algorithms. Since a greedy algorithm always chooses the best possible option available at the current time, without considering the future consequences or alternative choices, it would lead to suboptimal solutions under PSCs. Although there have been improved greedy algorithms such as those proposed in [6–8] designed for the PSCs, they still face challenges like computational burden, steady-state oscillations, and being trapped in a suboptimal solution. Usually, prior knowledge of P-V or power current (P-I) characteristics under PSCs is necessary to have these algorithms work under PSCs.

For AI methods, artificial neural networks (ANNs) [9,10] are the most commonly used methods to develop for MPPT. ANN consists of a series of neurons, which are organized into layers. The network attempts to learn the underlying relationship between the input and output by adjusting the weights of the network using an optimization algorithm such as gradient descent. The optimization algorithm tries to minimize the difference between the predicted output of the network and the actual output. However, they can be computationally intensive and require large amounts of data to train effectively.

MHAs are optimization techniques that are designed to efficiently explore large search spaces and find near-optimal solutions. These algorithms do not guarantee finding the global optimal solution but rather search for the best solution within a reasonable amount of time. MHAs can be further categorized into single solution and population based searches. Single-solution methods focus on modifying and improving a single candidate solution throughout the search. Population-based approaches maintain and improve multiple candidate solutions, often using population characteristics to guide the search. Hence, population based MHAs are usually based on swarm intelligence algorithms or bio-inspired algorithms. A common example of a single-solution MHA is the simulated annealing (SA) algorithm, which has been proposed for MPPT tracking by Lyden [11]. However, SA may take a long time to deliver the final solution if the cooling process is slow. For population-based MHAs, particle swarm optimization (PSO) was one of the first few methods to be implemented for MPPT [12]. and has been widely used to counteract the problem of PSCs due to its simple structure and easy implementation. However, PSO has some drawbacks, including long settling time and sustained PV output power oscillations during tracking. Consequently, other population based MHAs have been proposed for MPPT. These include grey wolf optimization (GWO) [13], firefly algorithm [14], ant colony optimization (ACO) [15], bat algorithm (BA) [16], Cuckoo search algorithm (CSA) [17], golden eagle optimization (GEO) [18], genetic algorithm [19] and et cetera. These methods although in some situations perform better than PSO, they still have similar problems of long searching time and being trapped in local optima. Therefore, researchers have further made modifications on these MHAs. The easiest approach is to combine a MHA with a deterministic approach (DA) such as P & O method because such a hybrid method can leverage the strengths of MHAs and DAs to find the GMPP. For example, Lian et al. [20] proposed a hybrid method, combining P & O with PSO. Initially, the P & O method is employed to allocate the nearest local maximum. Then, starting from that point on, the PSO method is employed to search for GMPP. Nugraha et al. [21] integrated the best aspects of the CSA and the golden section search (GSS) to leverage advantageous characteristics from both algorithms and use them as the MPPT control method for extracting the maximum power. Tomar et al. [22] proposed

a method that combines the crow search algorithm (CSA) and the perturb-and-observe method to increase tracking efficiency and reduce tracking time. Liao et al. [23] made enhancements to the BA by incorporating the abandonment mechanism from the CSA algorithm. The motivation behind this modification was that the original BA may struggle to locate the GMPP when there are local maximum power points (LMPPs) near the GMPP. The results of their study indicate that incorporating this modification can improve the convergence speed by approximately 35% across various PV curves. Abo-Khalil et al. [24] used SA for maximum power searching and then switched to P & O to attain a more precise convergence. Koh et al. [25] introduced a modified PSO technique, combined with an adaptive local algorithm. The approach utilizes a rank-based selection scheme to identify the top-performing half of the population, which is then employed in subsequent global and local search processes. Following that, a local search method is implemented, combining perturb and observe with an adaptive step size approach, to fine-tune the near-optimal duty cycle and achieve precise tracking of the GMPP. Nevertheless, a hybrid method is more complex to implement. Also, the transition criteria from a DA to a MHA and vice versa is sometimes difficult to define. Hence, another approach is to modify the existing MHAs. This includes modifying the search operators or the parameter settings, to enhance exploration or exploitation capabilities of MHAs. For example, one can introduce a new operator to diversify the search process or fine-tune the parameter values to balance exploration and exploitation. Ishaque et al. [26] proposed an improved MPPT method for the PV system using a modified PSO algorithm to reduce the steady-state oscillation once the GMPP is located. Makhoulfi et al. [27] presented a logarithmic PSO method for MPPT to reduce power oscillations during the search process and accelerates the convergence without search window reduction. Millah [28] improved the performance of the grey wolf optimization (GWO) by incorporating the pouncing actions and other weighting factors in the original GWO algorithm. The results demonstrated an enhancement in dynamic tracking efficiency of over 2% compared to the original GWO. Teshome et al. [29] modified the FA and used the average of all the brighter fireflies as the representative point so that the firefly only move toward this point without wandering toward all the brighter flies. Their method not only drastically decreases the tracking time and reduces the number of operations per iteration but also saves up to 67% of the tracking time, as compared with the original FA. Authors of [30] proposed an improved Rat Swarm Optimizer algorithm by initializing with detecting and skips method and employing an adaptive step size method for varying load. Overall, improving MHAs is an ongoing research topic for MPPT that requires a deep understanding of the optimization problem. This paper proposes a modified GEO for MPPT. The original GEO method does not take into account the fact that golden eagles engage in stooping behaviour when hunting small animals such as rodents, rabbits, or birds. Thus, the proposed method incorporates the stooping behaviour, which completes the true hunting behaviour of the golden eagle. The proposed method has been validated with experiments under various static and dynamic conditions. It will be shown that the developed GEO can lower the tracking time up to 42.41% and increase the dynamic efficiency more than 1.95%, compared to the original GEO. In addition, various state-of-the-art methods have also been compared with the proposed method, and it will be shown that the proposed method also outperform these methods.

The proposed method is an enhanced version of the GEO algorithm. The main contributions of the paper can be summarized as follows:

1. A new procedure, stooping, is added to the GEO to improve convergence speed in the late search period. Since a golden eagle may engage in stooping during hunting, this newly added procedure completes the GEO.
2. On average, the proposed method can reduce tracking time by 42.41% and improve dynamic tracking accuracy by 1.95%, compared to GEO.
3. The proposed method underwent thorough validation through rigorous experimentation using a PV emulator. A wide range of complex tests was conducted to simulate real-world dynamic changes in solar irradiance. The performance of the proposed

method was then compared to several state-of-the-art techniques. The results indicate the superiority of the proposed method, outperforming these techniques in both MPPT accuracy and tracking time.

The remaining sections of this paper are structured as follows. Section 2 describes GEO and details the development of the proposed method presented in this paper. Section 3 illustrates the results of the experiments. Finally, Section 4 concludes this paper.

2. Golden Eagle Optimization

2.1. Overview

The golden eagle, a member of the Accipitridae family, is one of the largest eagles in the world and can be found throughout the northern hemisphere, from Eurasia to North America. The golden eagle possesses remarkable hunting abilities, including exceptional eyesight, high-speed flight, and good hunting instinct, enabling it to capture prey of various sizes ranging from small rodents to medium-sized animals such as groundhogs or rabbits. In some instances, it even collaborates with other golden eagles to capture larger prey such as wolves or deer, which increases hunting efficiency and safety. The behavior of a golden eagle is unique and can be seen in Figure 1. It involves a spiral trajectory and two forces, which are the propensity to attack and the propensity to cruise.

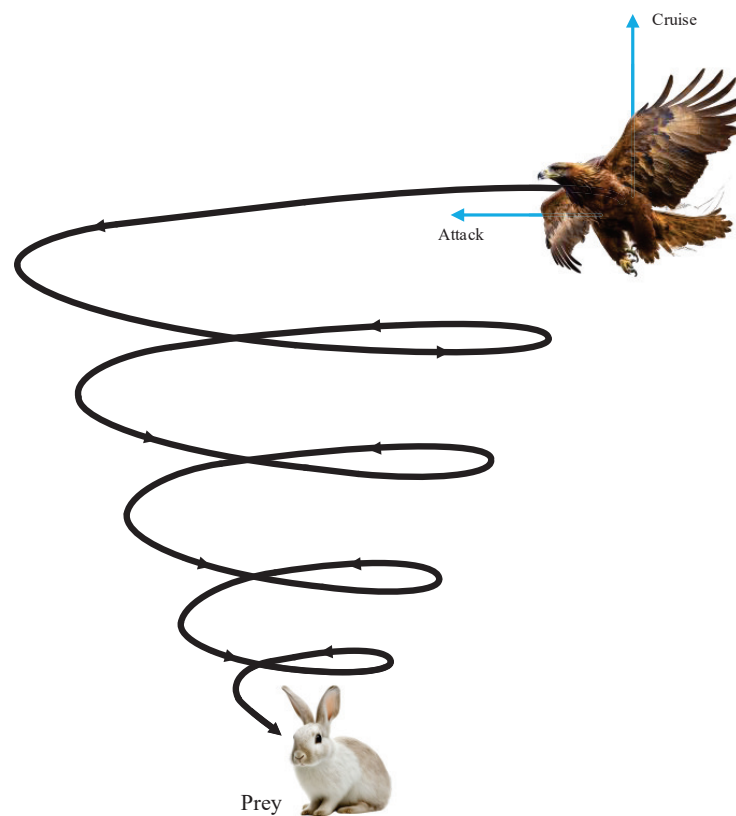


Figure 1. Habit behavior of golden eagles.

In GEO, we assume that golden eagles cooperate in hunting. While hunting, golden eagles start spiral trajectory behaviour, from exploration mode (low-attack and high-cruise propensities) to exploitation mode (high-attack and low-cruise propensities) smoothly. Each golden eagle starts its hunting behaviour by flying at high altitudes within its realm in large circles and beginning to search for the best prey. Once the prey is spotted, the golden eagle starts moving in a circle route where the prey is in the center and starts spiral trajectories of the exploration mode. If a golden eagle and other golden eagles do not spot another better prey, it will regard the current spotted prey as the best prey, sending the location

of the best prey to other golden eagles and switch hunting behaviour to the exploitation mode, continuing their spiral trajectory behaviour until reaching the location of the best prey to attack. If one golden eagle finds out that there is a prey better than the previous one during the reasonable searching time, it will abandon its previous choice and start to spot the new best prey, sending the location of the new best prey to other golden eagles. They will continue their spiral trajectories until the location of the new best prey is reached.

2.2. Mathematical Model

According to [31], the hunting behaviour of the golden eagle can be divided into two forces: attack and cruise. The GEO algorithm of the following equations are combined with these two elements to update the position of golden eagles.

2.2.1. Attack (Exploitation)

The attack force can be seen as a vector that expresses the eagerness to attack. This vector originates from the current position of the golden eagle and terminates at the location of the most desirable prey. It is possible to compute the attack vector for each golden eagle using the following equation:

$$\vec{A}_i = \vec{X}_f - \vec{X}_i, \quad (1)$$

where \vec{A}_i is an attack vector, \vec{X}_f represents the current global best prey's location among all golden eagles' hunting memory and \vec{X}_i means the current position of each golden eagle i .

2.2.2. Cruise (Exploration)

The cruise force can be regarded as a vector with cruise propensity. This vector is a tangent vector to the circle and perpendicular to the attack vector. The cruise vector for each golden eagle i can be stated as:

$$\vec{C}_i = [c_1 = random, c_2 = random, \dots, c_n = random] \quad (2)$$

where *random* is a random non-integral value between zero and one. The component of cruise vector is composed of random values.

2.2.3. Transition from Exploration to Exploitation

As mentioned before, in the initial stages, golden eagles show spiral trajectory behaviours in the exploration mode (low-attack and high-cruise propensity) for searching for the best prey and smoothly shift to the exploitation mode (high-attack and low-cruise propensity) to attack the best prey in the final stages. To verify the tendency of exploration and exploitation modes, we need to find out the characteristics of attack and cruise propensities. The propensity to attack and propensity to cruise can be calculated via (3) and (4):

$$p_a = p_a^0 + \frac{t}{T} | p_a^T - p_a^0 | \quad (3)$$

$$p_c = p_c^0 - \frac{t}{T} | p_c^T - p_c^0 | \quad (4)$$

where p_a represents the propensity to attack and p_c represents the propensity to cruise, t indicates current iteration times, and T indicates maximum iteration times. p_a^T and p_a^0 represent the parameters for attack propensity. p_c^T and p_c^0 represent the parameters for cruise propensity.

As shown in Figure 2, as iteration increases, the propensity to attack (p_a) is more intense while the propensity to cruise (p_c) is more inactive.

The propensity to attack, p_a and propensity to cruise, p_c can affect the convergence process. This can be seen in Figure 3. If we set initial values of p_c to be 60 and p_a to be

30, the convergence rate is better than the case when initial values of p_c to be 80 and p_a to be 40.

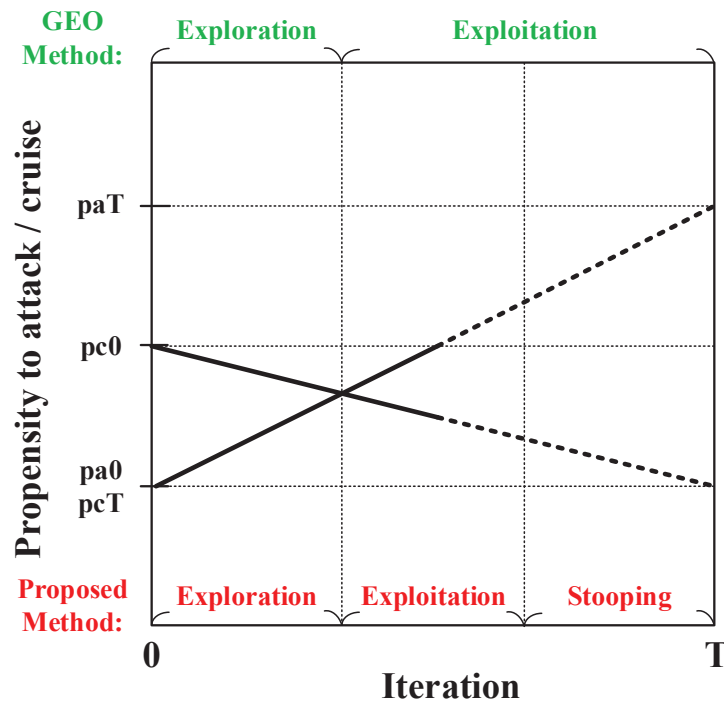


Figure 2. p_a and p_c over the course of iterations in GEO.

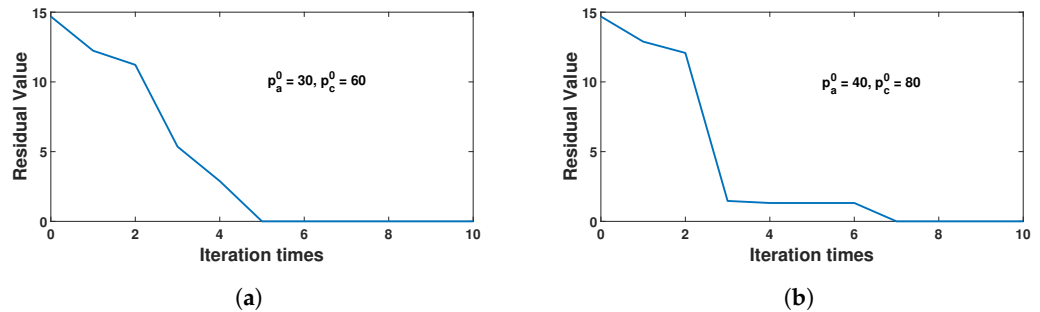


Figure 3. Initial values of p_a and p_c (a) $p_a^0 = 30$ and $p_c^0 = 60$; (b) $p_a^0 = 40$ and $p_c^0 = 80$.

2.2.4. Moving to New Positions

The incremental position of golden eagle i , Δx_i involves attack vector \vec{A}_i , cruise vector \vec{C}_i , propensity to attack p_a and propensity to cruise p_c . The calculation of Δx_i is as follows:

$$\Delta x_i = \vec{r}_1 p_a \frac{\vec{A}_i}{\|\vec{A}_i\|} + \vec{r}_2 p_c \frac{\vec{C}_i}{\|\vec{C}_i\|} \tag{5}$$

where $\|\vec{A}_i\|$ and $\|\vec{C}_i\|$ are the Euclidean norm of the attack and cruise vectors, as stated in (6). \vec{r}_1 and \vec{r}_2 are random vectors whose elements are non-integer and lie in the interval $[0, 1]$.

$$\|\vec{A}_i\| = \sqrt{\sum_{j=1}^n a_j^2}, \|\vec{C}_i\| = \sqrt{\sum_{j=1}^n c_j^2} \tag{6}$$

Hence, the position of golden eagle i in the next iteration, x_i^{t+1} can be calculated as

$$x_i^{t+1} = x_i^t + \Delta x_i^t \tag{7}$$

where x_i^t means the position of golden eagle i in the current iteration.

If one of the golden eagles finds out that there is a new prey better than the current global best prey, \vec{X}_f will be replaced by the new location of the new prey (the new global best prey) and the algorithms will restart the renew process for the next iteration. If a golden eagle finds out that the current global best prey is still the best, \vec{X}_f will remain to be the current global best prey and the algorithms will restart the renewal process for the next iteration.

2.3. Proposed Stooping Behaviour

“Stooping” refers to a hunting technique where an eagle will dive down toward its prey with incredible speed and force, as shown in Figure 4. This is often used to catch smaller animals like rodents or fish. To mathematically model stooping, we proposed to use (8).

$$x_i^{t+1} = \vec{X}_f \pm d, \quad (8)$$

where d is a random number generated in the interval $[0, a]$. Note that (8) is similar to the concept of the random walk in BA. The local search of the BA allows the bat to exploit the local search space to correct the best solution.

We proposed to switch to the stooping mode when one of the two conditions are satisfied.

1. An eagle is approximately close to the prey.
2. A certain iteration number is reached.

Since the prey (i.e., the GMPP) will not be known until the reaching condition is satisfied, the position of the prey can be approximated by the global best of the eagles. For the second condition, we divided the iteration process into exploration, exploitation, and stooping modes. As in the original GEO, the breakpoint between exploration and exploitation of the proposed method is when p_c and p_a intersects. Nevertheless, we proposed that transition from exploitation to stooping modes occurs when the area under p_c curve before the breakpoint is equal to the area above p_c after the breakpoint, as shown in Figure 2.

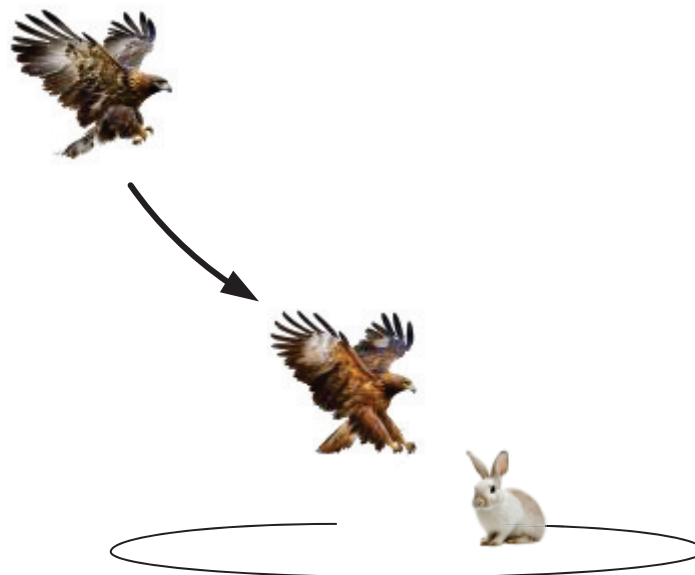


Figure 4. Stooping behavior of golden eagle.

2.4. Benchmark Functions Test

The proposed algorithm is tested on the benchmark functions as proposed in [32]. These benchmark functions are commonly used to test the performance of a MHA. They are minimization functions and can be divided into three groups: unimodal (F_1 – F_7), multimodal (F_8 – F_{16}), fixed-dimension multimodal (F_{14} – F_{23}). The statistical results (average and standard deviation) are reported in Table 1. The proposed method outperforms or ties with the golden eagle optimization (GEO) in 18 functions out of 23. Also, the proposed method performed exceptionally well on multimodal and fixed-dimension multimodal functions.

Table 1. Optimization results obtained by GEO and the proposed method on the 23 benchmark functions. (✓: proposed method outperforms GEO; Δ: proposed method ties with GEO).

	GEO		Proposed Method	
	Mean	Std	Mean	Std
F_1 ✓	9.24×10^{-34}	4.89×10^{-33}	0	0
F_2	7.94×10^{-94}	3.05×10^{-93}	1.32×10^{-83}	4.09×10^{-83}
F_3	1.35×10^{-125}	3.58×10^{-125}	4.33×10^{-112}	9.41×10^{-112}
F_4 Δ	−1.00	0	−1.00	0
F_5	−4.89	4.78×10^{-3}	−4.87	1.14×10^{-2}
F_6	1.78×10^{-11}	1.03×10^{-11}	5.70×10^{-11}	2.44×10^{-11}
F_7	4.92×10^{-14}	1.76×10^{-14}	6.81×10^{-14}	2.19×10^{-14}
F_8 Δ	−1.00	0	−1.00	0
F_9 Δ	-9.60×10^2	0	-9.60×10^2	0
F_{10} Δ	0	0	0	0
F_{11} Δ	1.35×10^{-31}	0	1.35×10^{-31}	0
F_{12} ✓	6.90×10^{-1}	6.81×10^{-1}	4.32×10^{-6}	1.59×10^{-6}
F_{13} ✓	1.09×10^{-2}	9.75×10^{-3}	5.35×10^{-6}	2.32×10^{-6}
F_{14} ✓	2.51×10^{-1}	5.13×10^{-2}	1.74×10^{-1}	2.40×10^{-2}
F_{15} ✓	−8.93	3.87×10^{-1}	−9.51	1.04×10^{-1}
F_{16} ✓	3.81×10^{-2}	5.66×10^{-2}	2.16×10^{-7}	2.20×10^{-7}
F_{17} ✓	1.06×10^{-2}	3.35×10^{-3}	3.58×10^{-8}	3.01×10^{-8}
F_{18} ✓	2.68	2.61×10^{-1}	1.57	2.74×10^{-1}
F_{19} ✓	1.16	2.20	1.05×10^{-1}	5.70×10^{-2}
F_{20} ✓	1.23×10^1	3.15	6.60	1.30
F_{21} ✓	4.00	7.71	1.02×10^{-1}	5.38×10^{-2}
F_{22} ✓	4.20×10^{-1}	4.00×10^{-2}	2.97×10^{-1}	1.80×10^{-2}
F_{23} ✓	3.66×10^{-20}	3.60×10^{-20}	6.04×10^{-21}	2.40×10^{-21}

3. Experimental Setup and Test Result

For the experiment, we carry out one static case and three dynamic cases. The static case means that no continuous P-V curve is changing and there are four different static P-V curves to be tested, as shown in Figure 5. The first dynamic case means that algorithms of MPPT are tested with a sequence of continuously changing P-V curves. The second dynamic case means algorithms of MPPT are tested with a reversed sequence of continuous P-V curves. The third dynamic case means algorithms of MPPT are tested with continuous P-V curves whose GMPPs are largely different. During the GMPP tracking experiment, a group of five eagles was employed. It was noticed that increasing the number of eagles had the potential to improve accuracy; however, it also resulted in longer search times and higher computational demands. After conducting several offline simulations, it was determined that utilizing five eagles achieved a favorable balance between tracking efficiency and time. The initial values for these five search agents were set at 90%, 75%, 60%, 45%, and 30% of the open circuit voltage. To ensure a fair comparison, all algorithms were applied with the same initial conditions for both static and dynamic scenarios.

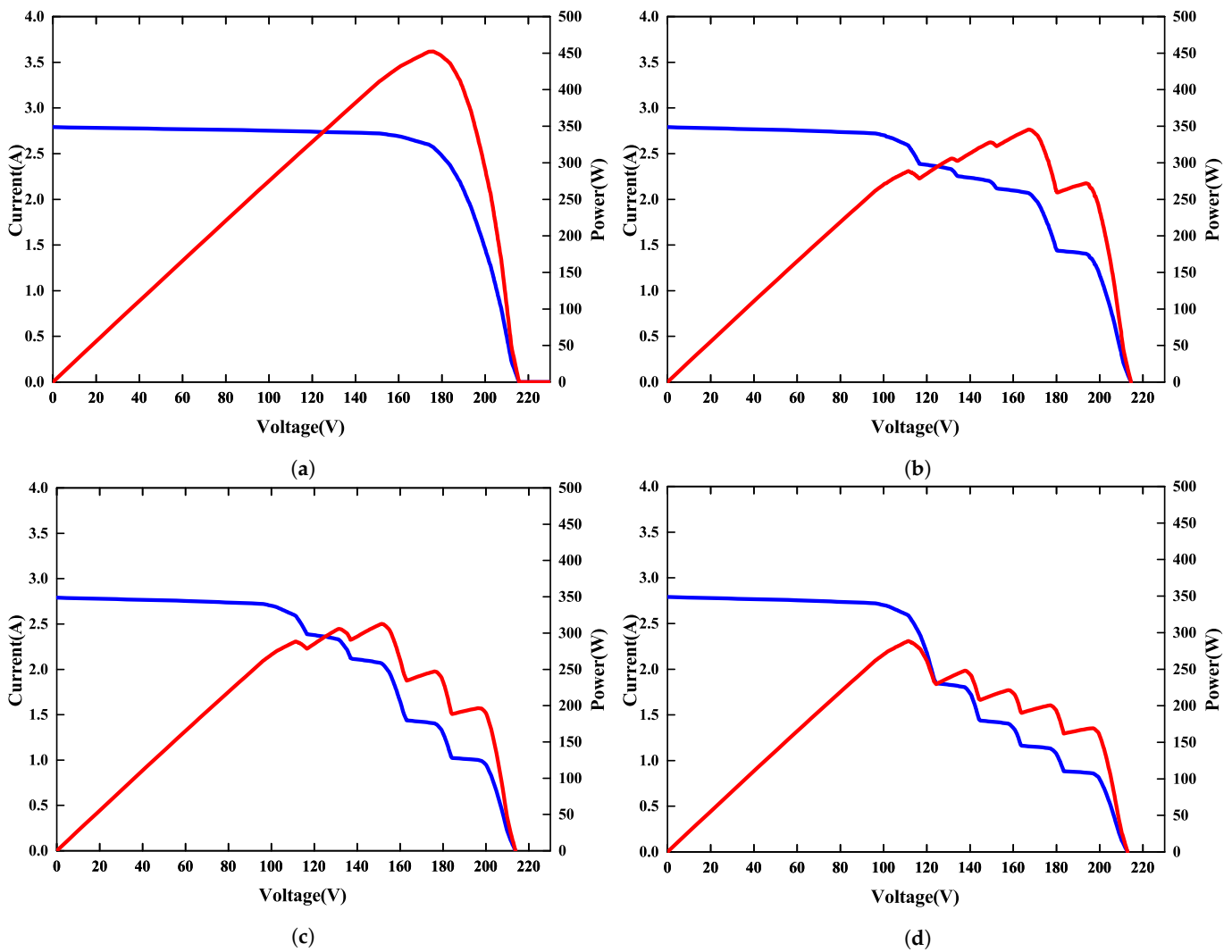


Figure 5. P-V curves for (a) scenario 1; (b) scenario 2; (c) scenario 3; (d) scenario 4.

3.1. Experimental Setup

The experimental configuration consists of a programmable P-V emulator, a digital signal processor, an interleaved DC-DC boost converter, and a DC power supply, as shown in Figure 6.

The programmable P-V emulator (AMETEK ETS600X8C-PVF) can simulate various PV panel models for all circumstances, including PSCs. The MPPT control algorithm is implemented in the digital signal processor from Texas Instruments (TMS320F28035). The interleaved DC-DC boost converter comprises two pairs of inductors, diodes, and power switches and is more efficient than traditional DC-DC boost converters, with low input current and low output voltage ripple. Additionally, it can reduce element requirements, the electromagnetic interference, and boost transient response.

It is to be noted that the interleaved boost converter employed in this paper is to reduce current ripples. Thus, the two branches shown in Figure 7 are switched in a complementary fashion. The proposed enhanced GEO method is employed to track the GMPP. This is different from the approach used in [33,34] where the authors proposed to use interleaved converters to remedy the partial shading effects by extracting the summation of individual maximum power available from each PV array branches. In fact, different duty cycles are provided for each branch of the interleaved converter where a separate MPP tracker is used for each PV array to track its unique MPP.

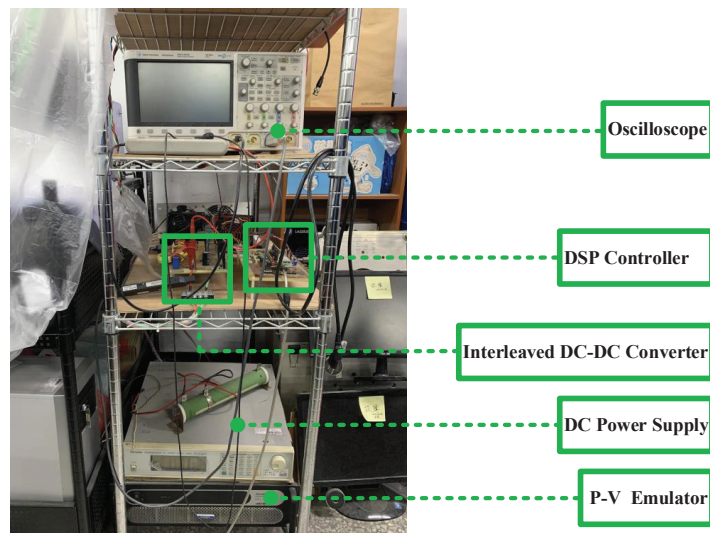


Figure 6. PV system experimental setup.

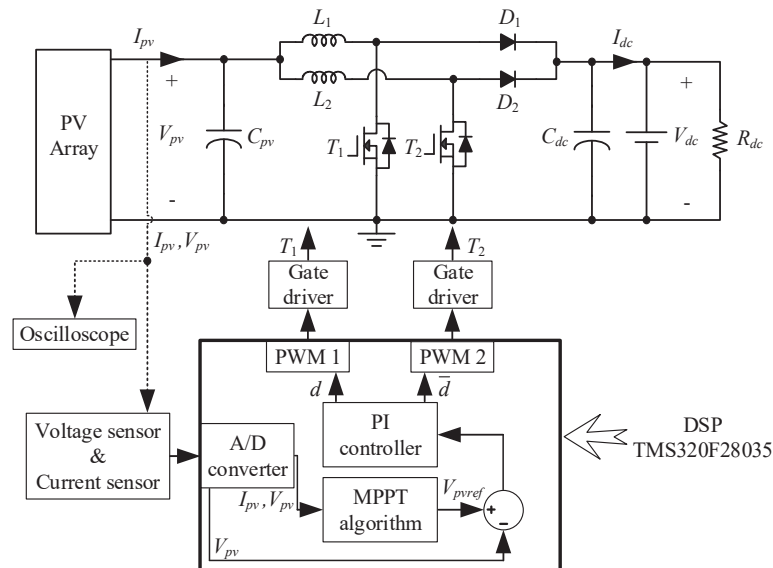


Figure 7. PV system schematic.

Table 2 is the characteristic and specifications of the solar module that the PV emulator mimics and Table 3 lists the hardware information of the experimental setup shown in Figure 7.

Table 2. Electrical parameters of ecoSology ECO300A156M-72 solar panel.

Solar module	ecoSology ECO300A156M-72
P_{max}	300 W
No. of cells, N_{cells}	72
V_{oc}	45.73 V
I_{sc}	8.71 A
V_{mp}	37.12 V
I_{mp}	8.09 A

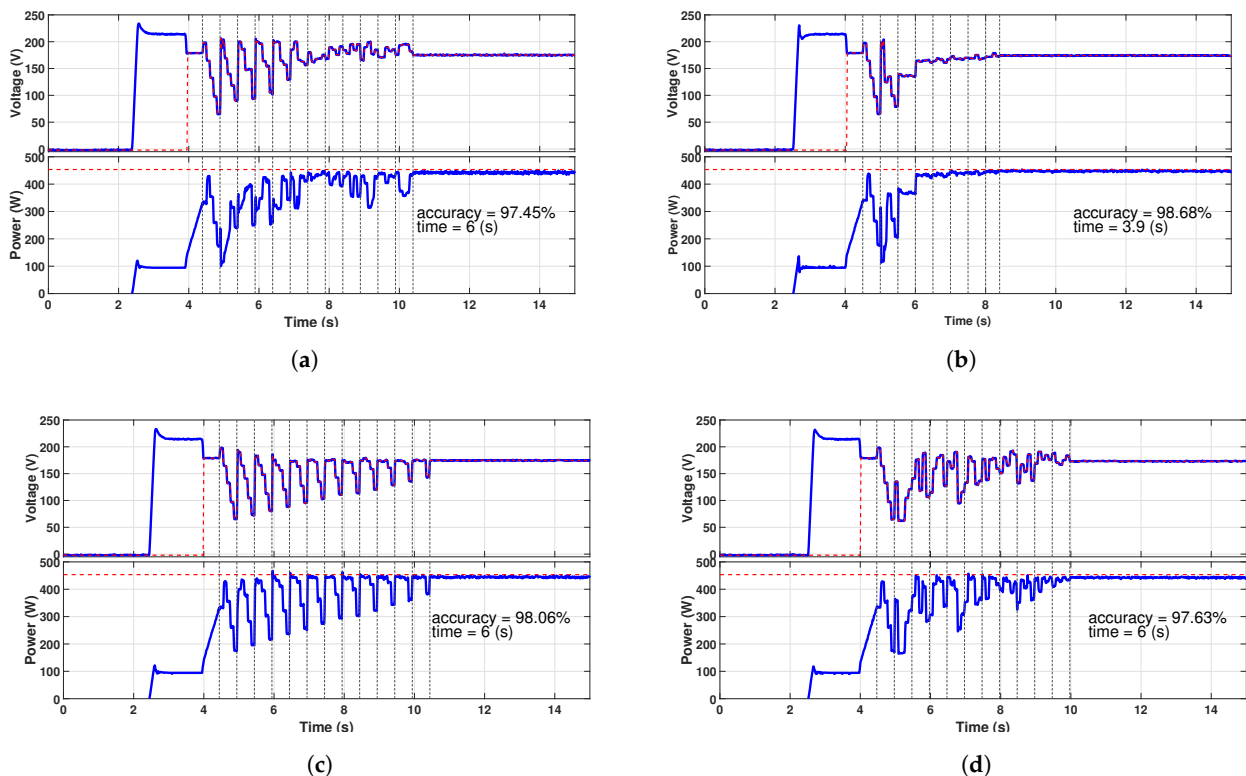
Table 3. Component data and operation range of the interleaved boost converter.

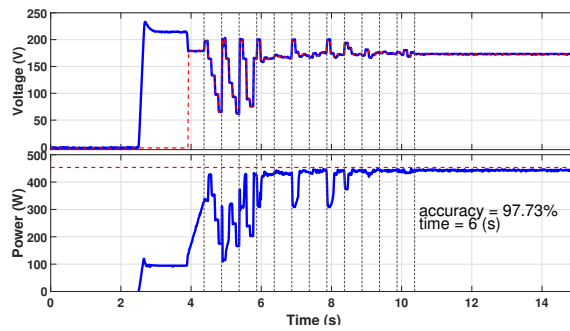
V_{pv}	0–224 V	Diode D_1	DSEI30-06A
V_{dc}	0–450 V	Diode D_2	DSEI30-06A
I_{pv}	0–2.8 A	L_1	2 mH
I_{dc}	0–1.43 A	L_2	2 mH
MOSFET T_1	17N80C3	C_{pv}	120 μ F
MOSFET T_2	17N80C3	C_{dc}	470 μ F
Switching frequency	100 kHz	Sampling frequency	100 kHz
Load, R_{dc}	350 Ω	Load power	600 W

3.2. Results of Static Cases

Figure 8a shows the tracking profile of the voltage and power of GEO for scenario 1. As shown in the figure, it takes a total of 12 iterations to reach the GMPP, leading to 6 s of tracking time, and the accuracy is 97.45%. On the other hand, Figure 8b shows that it only takes 8 iterations for the proposed method to reach the GMPP, leading to 3.9 s of tracking time, and the accuracy is 98.68%. The tracking profiles of PSO, GWO, and BA shown in Figure 8c–e, indicate that their efficiencies are smaller than the proposed method, and the tracking times are larger than that of the proposed method.

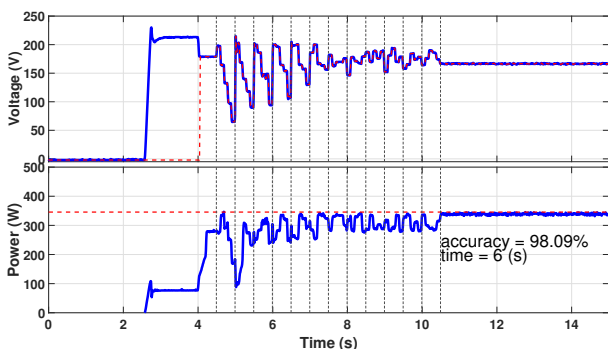
Figure 9a shows the tracking profiles of the power and voltage of GEO for scenario 2. As indicated in the figure, the tracking time and accuracy are 6 s and 98.09%, respectively. On the other hand, the tracking time and accuracy of the proposed method are 2.6 s and 99.18%, respectively, as shown in Figure 9b, demonstrating a much shorter tracking time and better accuracy, as compared to those of GEO. Figure 9c–e show the tracking profiles of PSO, GWO, and BA for scenario 2. As these figures indicate, the tracking times for PSO, GWO, and BA are 6 s, 4.4 s, and 6 s, respectively, which are much longer than that of the proposed method. Also, the tracking accuracies of PSO, GWO, and BA are 98.7%, 98.06%, and 98.93%, respectively, which are also lower than that of the proposed method. The tracking profiles of various algorithms for scenarios 3 and 4 are in general similar to those of scenarios 1 and 2.

**Figure 8.** Cont.

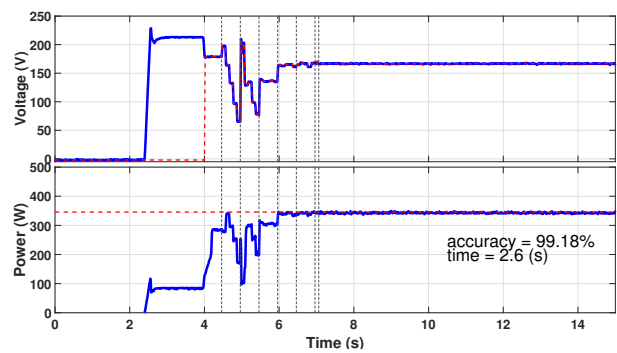


(e)

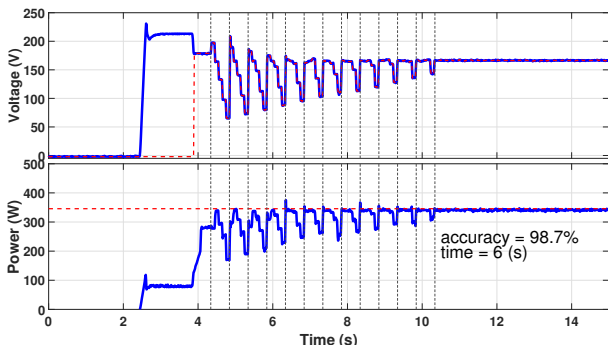
Figure 8. Voltage and power waveforms for scenario 1: (a) GEO; (b) the proposed method; (c) PSO; (d) GWO; (e) BA.



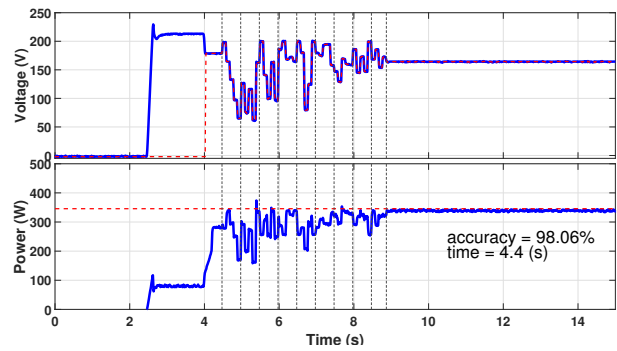
(a)



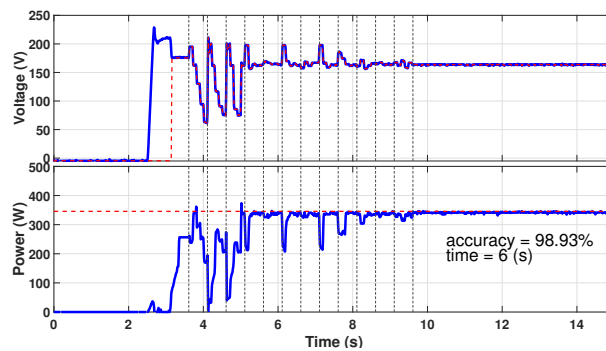
(b)



(c)



(d)



(e)

Figure 9. Voltage and power waveforms for scenario 2: (a) GEO; (b) the proposed method; (c) PSO; (d) GWO; (e) BA.

As shown in Table 4, on average, the proposed algorithm performs with the highest accuracy, followed by GEO, PSO, GWO, and BA. Their accuracies are 98.64%, 98.41%, 98.01%, 97.82%, and 97.73%, respectively. For the MPPT tracking times, as shown in Table 4, on average, the proposed method performs with the shortest MPPT tracking time, followed by PSO, GWO, GEO, and BA. Their tracking times are 3.3 s, 4.05 s, 5.73 s, 5.5 s, and 5.99 s, respectively. In other words, the proposed method spent on average only 57.59% of the tracking time, of the GEO. Compared to PSO, the proposed method spends only 81.48% of PSO's tracking time.

Table 4. Static case result.

Method		GEO	Proposed	PSO	GWO	BA
Scenario 1	accuracy	98.4% \pm 0.05	98.85% \pm 0.205	98.16% \pm 0.059	98.37% \pm 0.043	97.87% \pm 0.088
	time	5.56 \pm 0.7 (s)	3.31 \pm 0.342 (s)	3.23 \pm 0.485 (s)	5.49 \pm 0.064 (s)	5.98 \pm 0.073 (s)
Scenario 2	accuracy	98.82% \pm 0.081	99.05% \pm 0.383	98.12% \pm 0.063	98.16% \pm 0.02	97.89% \pm 0.041
	time	5.96 \pm 0.01 (s)	3.12 \pm 0.29 (s)	3.95 \pm 0.129 (s)	5.49 \pm 0.045 (s)	5.98 \pm 0.104 (s)
Scenario 3	accuracy	99.18% \pm 0.379	98.63% \pm 0.1	98.14% \pm 0.078	97.09% \pm 0.09	97.87% \pm 0.045
	time	5.43 \pm 0.487 (s)	3.29 \pm 0.227 (s)	3.93 \pm 0.423 (s)	5.49 \pm 0.037 (s)	5.99 \pm 0.149 (s)
Scenario 4	accuracy	97.24% \pm 0.267	98.03% \pm 0.132	97.63% \pm 0.029	97.68% \pm 0.086	97.3% \pm 0.032
	time	5.97 \pm 0.005 (s)	3.49 \pm 0.69 (s)	5.082 \pm 0.361 (s)	5.51 \pm 0.029 (s)	6.01 \pm 0.126 (s)
Average	accuracy	98.41%	98.64%	98.01%	97.82%	97.73%
	time	5.73 (s)	3.3 (s)	4.05 (s)	5.5 (s)	5.99 (s)

3.3. Dynamic Case Result

A total of seven P-V curves are generated to test the algorithms' capabilities for continuous dynamic tracking. Figure 10 displays the sequence of the P-V curves.

Based on [35], there are two ways of re-initialization for a maximum power tracker. The first method depends on dispersing the particles at a certain predefined time in order to look for the new GMPP of a new partial shading condition. The second one is to continually monitor any changes in partial shading conditions to disperse the particles to follow the new GMPP. We have actually adapted the second method.

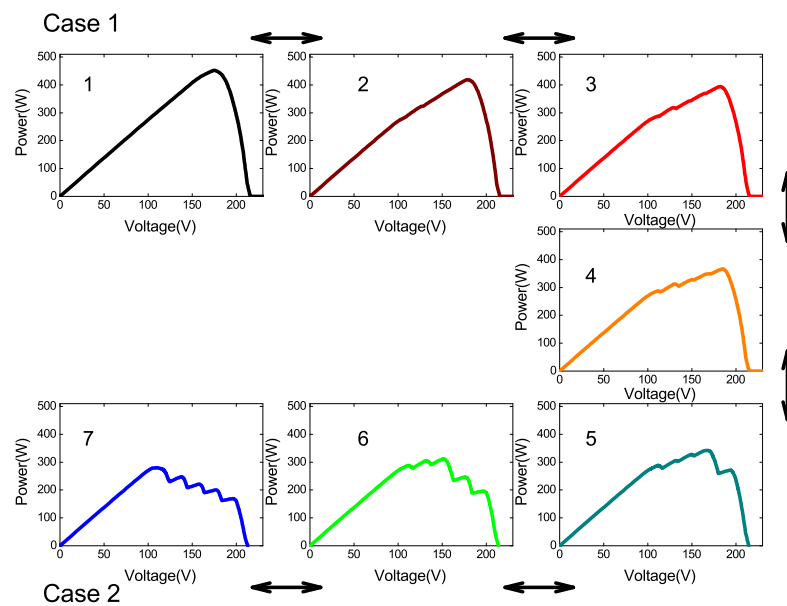


Figure 10. P-V curves for the dynamic cases.

Note that the non-uniform P-V curve is not covered by the European test standard EN50530 [36], which is only applicable to the uniform P-V curve. Tracking non-uniform

P-V curves takes more time. However, the irradiance change rate, defined by the EN50530 European test standard are too quick to notice. We use 12 s as the change time to give each algorithm enough time to adequately settle before testing how well they perform under non-uniform P-V curve conditions.

According to [36], the following equation can be used to determine the effectiveness of dynamic tracking:

$$\eta_d = \frac{\sum_i V_{pv,i} \cdot I_{pv,i} \cdot \Delta T_i}{\sum_j GMP_{th,j} \cdot \Delta T_j} \times 100\% , \quad (9)$$

where ΔT_i is the time in which the $V_{pv,i}$ and $I_{pv,i}$ are sampled and ΔT_j is the period in which the $GMP_{th,j}$ is delivered.

To detect the variance in P-V curves of GMPPs [29], an extra condition is needed, as mentioned in (10).

$$\frac{|P_{pv} - P_{pv,last}|}{P_{pv,last}} \geq \Delta P_{pv}, \quad (10)$$

where $P_{pv,last}$ is the previously found GMPP and ΔP_{pv} is set to 6%. After $P_{pv,last}$ is found, the setup will restart to track the new GMPP if the condition is detected.

Note that if the difference in power is less than the tolerance value, then the new GMPP will probably be missed. However, such a problem would also impose difficulty for most of the existing MPPT method and is beyond the scope of this paper.

3.3.1. Dynamic Case 1

Figure 11a–e are voltage and power waveforms of the GEO, proposed method, PSO, GWO, and BA, respectively. From Figure 11a–e, all of the algorithms can track the GMPPs from curve 1 to curve 7 successfully. However, the dynamic tracking accuracy can be quite different. As shown in Table 5, the proposed algorithm performs with the highest dynamic tracking accuracy, followed by GEO, PSO, GWO, and BA, which are 96.79%, 94.82%, 94.62%, 92.93%, and 91.97%, respectively. The proposed method performs the best in terms of tracking the maximum point in each sequence and achieves a high level of accuracy in attaining the GMPP.

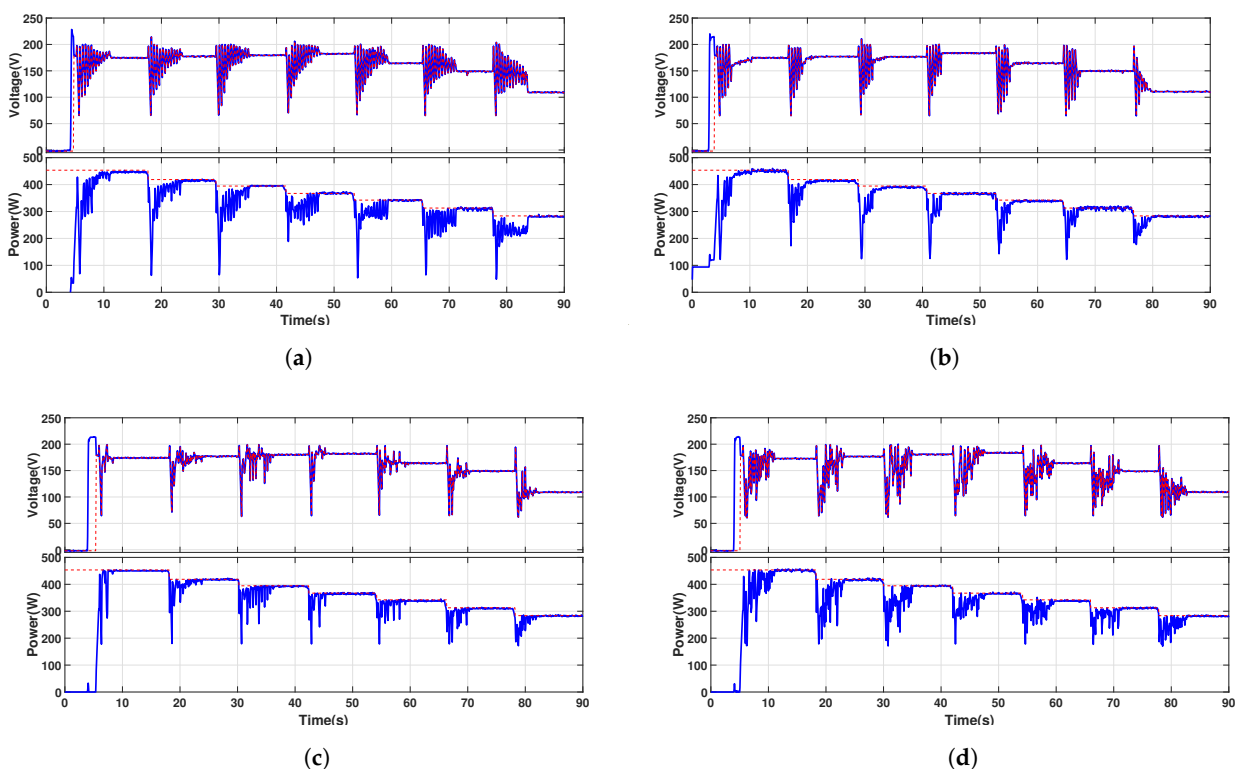
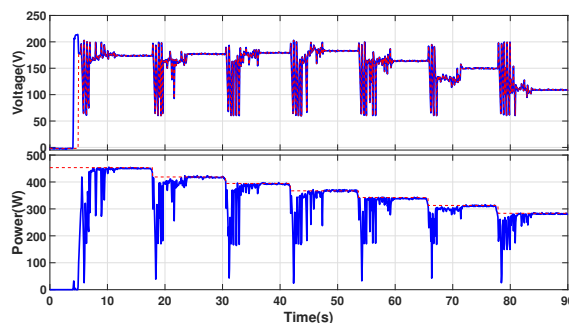


Figure 11. Cont.



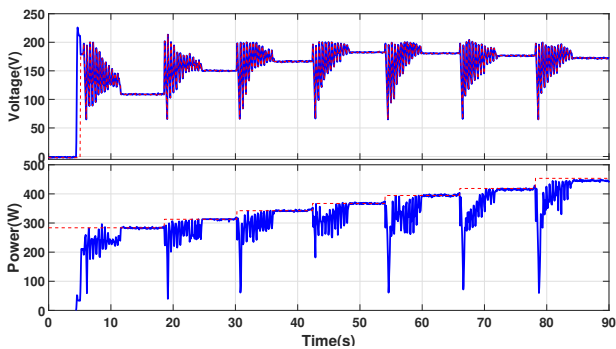
(e)

Figure 11. Voltage and power waveforms for dynamic case 1: (a) GEO; (b) the proposed method; (c) PSO; (d) GWO; (e) BA.

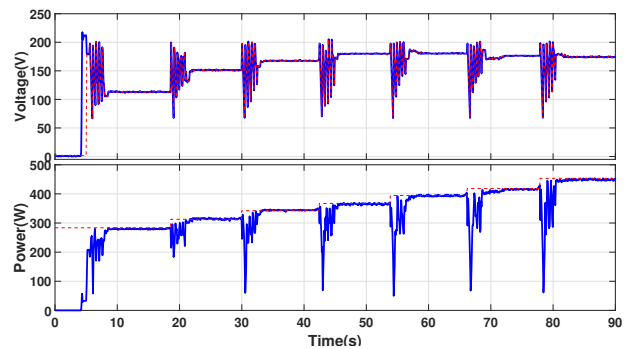
3.3.2. Dynamic Case 2

This case also includes seven P-V curves, which are identical to the curves used in the first dynamic case. However, the sequence in which the curves evolve is reversed. The P-V profiles displayed in Figure 10 are difficult to track and are useful for testing MPPT control algorithms since all profiles undergo gradual changes. The change of P-V curves is also detected by (10), as mentioned before.

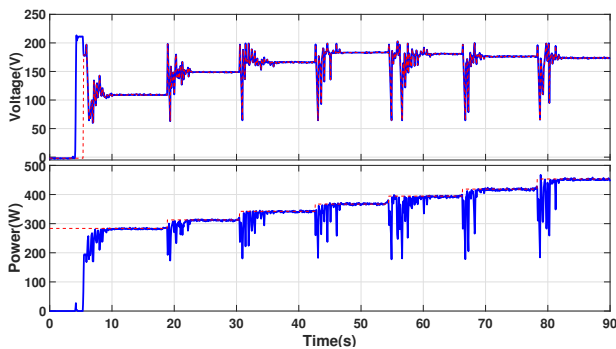
Figure 12a–e are voltage and power waveforms of the GEO, proposed method, PSO, GWO, and BA, respectively. As shown in Table 5, the proposed algorithm performs with the highest dynamic tracking accuracy, followed by GEO, PSO, GWO, and BA, which are 98.13%, 96%, 94.39%, 93.09%, and 92.47%, respectively. The proposed algorithm also outperforms the other algorithms in the reverse tracking case because it has the shortest tracking time and attains the GMPP with high accuracy, resulting in the best dynamic accuracy.



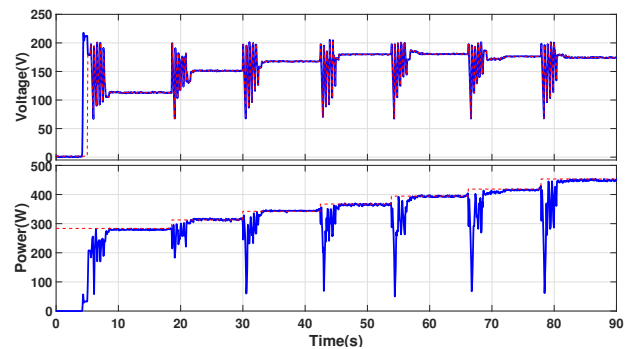
(a)



(b)

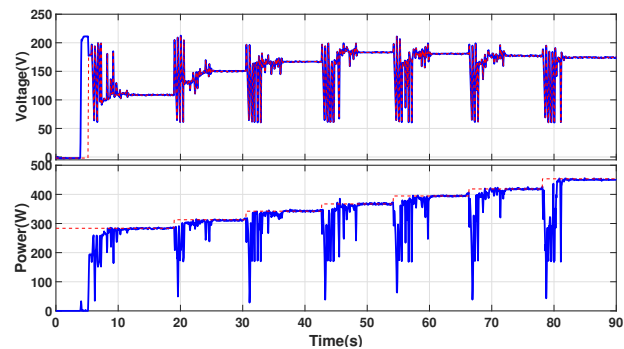


(c)



(d)

Figure 12. Cont.



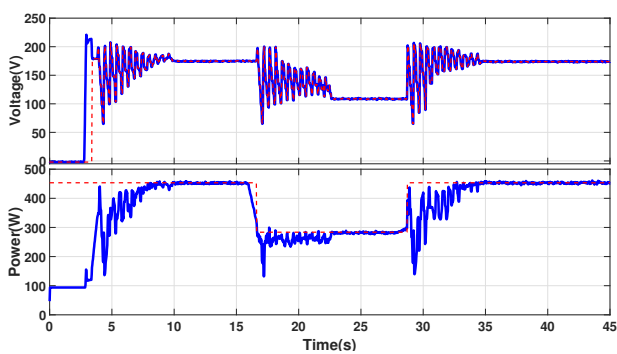
(e)

Figure 12. Voltage and power waveforms for dynamic case 2: (a) GEO; (b) the proposed method; (c) PSO; (d) GWO; (e) BA.

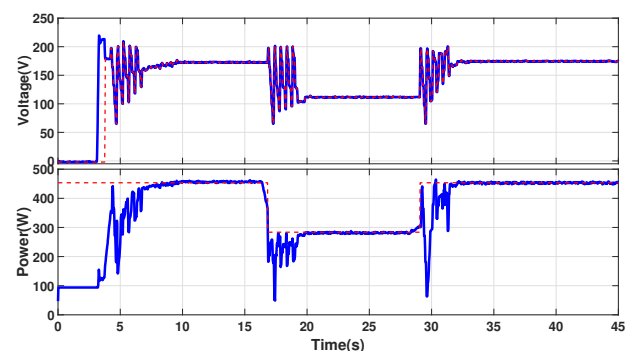
3.3.3. Dynamic Case 3

Compared to the first and second dynamic cases, this case consists of a very sharp power change. The starting power level is 453.38 W, the halfway power level is 283.63 W and the ending power level is back to 453.38 W. The evolving sequence of the curves is also illustrated in Figure 10, and the change of P-V curves is also detected in (10).

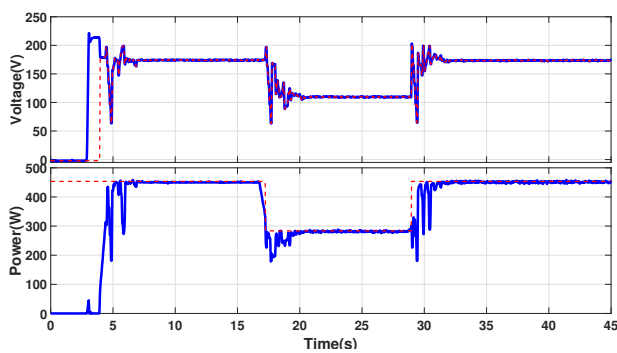
Figure 13a–e are voltage and power waveforms of the GEO, proposed method, PSO, GWO, and BA, respectively. As shown in Table 5, the proposed algorithm performs with the highest dynamic tracking accuracy, followed by GEO, GWO, PSO, and BA, which are 95.01%, 93.24%, 93.23%, 92.93%, and 92.75%, respectively.



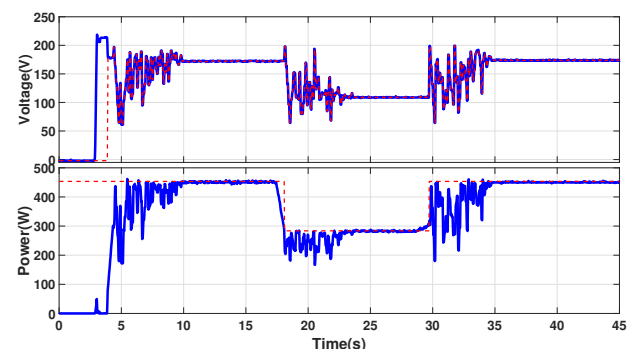
(a)



(b)

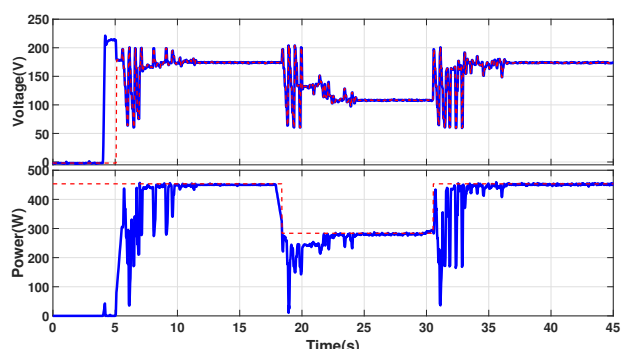


(c)



(d)

Figure 13. Cont.



(e)

Figure 13. Voltage and power waveforms for dynamic case 3: (a) GEO; (b) the proposed method; (c) PSO; (d) GWO; (e) BA.

As shown in Table 5, on average, the proposed algorithm performs with the highest dynamic tracking accuracy, followed by GEO, PSO, GWO, and BA, which are 96.64%, 94.69%, 93.98%, 93.08%, and 92.4%, respectively. In other words, the dynamic tracking accuracy on average can be enhanced by 1.95%, as compared to the original GEO. And the dynamic tracking accuracy on average can be enhanced by 2.66%, as compared to PSO. Also, on average, an improvement of 3.56% and 4.24% in dynamic tracking accuracy can be achieved by the proposed method, as compared to GWO and BA, respectively.

Table 5. Results of dynamic cases.

Algorithm	GEO	Proposed	PSO	GWO	BA
Case 1	94.82%	96.79%	94.62%	92.93%	91.97%
Case 2	96%	98.13%	94.39%	93.09%	92.47%
Case 3	93.24%	95.01%	92.93%	93.23%	92.75%
Average	94.69%	96.64%	93.98%	93.08%	92.4%

Furthermore, the findings of Section 3.2 indicate that the proposed method generally outperforms algorithms such as PSO, GWO, and BA due to the reasons outlined below:

1. Better exploration and exploitation: The proposed method inherited from GEO can effectively explore the solution space by employing the cruise behaviour while also exploiting promising areas by attacking and stooping.
2. Dynamic parameter adaptation: GEO includes mechanisms for dynamically adapting its control parameters during the optimization process. This adaptability helps the algorithm adjust its behaviour according to the problem's characteristics or changing conditions, leading to potentially improved convergence and robustness.
3. Powerful exploitation phase: The stooping behaviour of eagles is known for its efficiency in capturing prey. Similarly, The proposed method employs stooping behaviour in the promising regions by focusing its search on those areas, which can result in faster convergence and better exploitation of the best solutions in the optimization process.

4. Conclusions

This study has proposed a GEO-based approach with stooping behaviour, for maximum power point tracking. The performance of proposed method is compared with those of the GEO, PSO, GWO, and BA in terms of tracking accuracy and tracking time, and the results of the static experiment show that the proposed algorithm can achieve high accuracy while significantly reducing the tracking time. When compared with the GEO algorithm, the proposed method can save on average, 42.41% of the tracking time. In comparison with PSO, the proposed method can save an average of 18.52% of the tracking time. Furthermore, in various dynamic cases, the proposed algorithm can enhance the dynamic tracking

accuracy by 1.95%, 2.66%, 3.56%, and 4.24% as compared to the GEO, PSO, GWO, and BA, respectively.

Author Contributions: The research was carried out successfully with contribution from all authors. The main research idea, case scenario studies, and the design of experimental setup were contributed by K.-L.L. and Z.-K.F. contributed to the implementation of simulation and experiment, and the analysis of these data. J.-F.L. partially contributed to the implementation of the experiment and simulation. Z.-K.F., J.-F.L. and K.-L.L. have mainly contributed to the preparation of the manuscript. All authors have read and agreed to the published version of the manuscript.

Funding: This work was supported in part by the Ministry of Science and Technology (MOST), Taiwan, under Grant MOST 109-3116-F-006-019-CC1, and in part by the Taiwan Building Technology Center from the Featured Areas Research Center Program within the framework of the Higher Education Sprout Project by the Ministry of Education in Taiwan.

Acknowledgments: The author would like to sincerely thank the editor and anonymous reviewers for their valuable comments and suggestions, improving the quality of the article.

Conflicts of Interest: The authors declare no conflict of interest.

References

- Petrone, G.; Spagnuolo, G.; Teodorescu, R.; Veerachary, M.; Vitelli, M. Reliability Issues in Photovoltaic Power Processing Systems. *IEEE Trans. Ind. Electron.* **2008**, *55*, 2569–2580. [\[CrossRef\]](#)
- Jones, D.C.; Erickson, R.W. Probabilistic Analysis of a Generalized Perturb and Observe Algorithm Featuring Robust Operation in the Presence of Power Curve Traps. *IEEE Trans. Power Electron.* **2013**, *28*, 2912–2926. [\[CrossRef\]](#)
- Pilawa-Podgurski, R.C.N.; Li, W.; Celanovic, I.; Perreault, D.J. Integrated CMOS Energy Harvesting Converter with Digital Maximum Power Point Tracking for a Portable Thermophotovoltaic Power Generator. *IEEE J. Emerg. Sel. Top. Power Electron.* **2015**, *3*, 1021–1035. [\[CrossRef\]](#)
- Alajmi, B.N.; Ahmed, K.H.; Finney, S.J.; Williams, B.W. Fuzzy-Logic-Control Approach of a Modified Hill-Climbing Method for Maximum Power Point in Microgrid Standalone Photovoltaic System. *IEEE Trans. Power Electron.* **2011**, *26*, 1022–1030. [\[CrossRef\]](#)
- Hsieh, G.; Hsieh, H.; Tsai, C.; Wang, C. Photovoltaic Power-Increment-Aided Incremental-Conductance MPPT With Two-Phased Tracking. *IEEE Trans. Power Electron.* **2013**, *28*, 2895–2911. [\[CrossRef\]](#)
- Ahmed, J.; Salam, Z. An Enhanced Adaptive P & O MPPT for Fast and Efficient Tracking under Varying Environmental Conditions. *IEEE Trans. Sustain. Energy* **2018**, *9*, 1487–1496. [\[CrossRef\]](#)
- Manoharan, P.; Subramaniam, U.; Babu, T.S.; Padmanaban, S.; Holm-Nielsen, J.B.; Mitolo, M.; Ravichandran, S. Improved Perturb Observation Maximum Power Point Tracking Technique for Solar Photovoltaic Power Generation Systems. *IEEE Syst. J.* **2020**, *15*, 3024–3035. [\[CrossRef\]](#)
- Sun, Z.; Jang, Y.; Bae, S. Optimized Voltage Search Algorithm for Fast Global Maximum Power Point Tracking in Photovoltaic Systems. *IEEE Trans. Sustain. Energy* **2023**, *14*, 423–441. [\[CrossRef\]](#)
- Roy, R.B.; Rokonuzzaman, M.; Amin, N.; Mishu, M.K.; Alahakoon, S.; Rahman, S.; Mithulananthan, N.; Rahman, K.S.; Shakeri, M.; Pasupuleti, J. A Comparative Performance Analysis of ANN Algorithms for MPPT Energy Harvesting in Solar PV System. *IEEE Access* **2021**, *9*, 102137–102152. [\[CrossRef\]](#)
- Allahabadi, S.; Iman-Eini, H.; Farhangi, S. Fast Artificial Neural Network Based Method for Estimation of the Global Maximum Power Point in Photovoltaic Systems. *IEEE Trans. Ind. Electron.* **2022**, *69*, 5879–5888. [\[CrossRef\]](#)
- Lyden, S.; Haque, M.E. A Simulated Annealing Global Maximum Power Point Tracking Approach for PV Modules under Partial Shading Conditions. *IEEE Trans. Power Electron.* **2016**, *31*, 4171–4181. [\[CrossRef\]](#)
- Miyatake, M.; Veerachary, M.; Toriumi, F.; Fujii, N.; Ko, H. Maximum Power Point Tracking of Multiple Photovoltaic Arrays: A PSO Approach. *IEEE Trans. Aerosp. Electron. Syst.* **2011**, *47*, 367–380. [\[CrossRef\]](#)
- Mohanty, S.; Subudhi, B.; Ray, P.K. A New MPPT Design Using Grey Wolf Optimization Technique for Photovoltaic System under Partial Shading Conditions. *IEEE Trans. Sustain. Energy* **2016**, *7*, 181–188. [\[CrossRef\]](#)
- Sundareswaran, K.; Peddapati, S.; Palani, S. MPPT of PV Systems under Partial Shaded Conditions through a Colony of Flashing Fireflies. *IEEE Trans. Energy Convers.* **2014**, *29*, 463–472. [\[CrossRef\]](#)
- Besheer, A.; Adly, M. Ant colony system based PI maximum power point tracking for stand alone photovoltaic system. In Proceedings of the 2012 IEEE International Conference on Industrial Technology, Athens, Greece, 19–21 March 2012; pp. 693–698. [\[CrossRef\]](#)
- Eltamaly, A.M.; Al-Saud, M.S.; Abokhalil, A.G. A Novel Bat Algorithm Strategy for Maximum Power Point Tracker of Photovoltaic Energy Systems under Dynamic Partial Shading. *IEEE Access* **2020**, *8*, 10048–10060. [\[CrossRef\]](#)
- Ahmed, J.; Salam, Z. A Maximum Power Point Tracking (MPPT) for PV system using Cuckoo Search with partial shading capability. *Appl. Energy* **2014**, *119*, 118–130. [\[CrossRef\]](#)

18. Khan, Z.A.; Akhter, S.F.; Islam, S.; Abid, F. A Golden Eagle Optimization Based MPPT Control For Partial Shading Conditions. In Proceedings of the 2022 IEEE International Conference on Power Electronics, Smart Grid, and Renewable Energy (PESGRE), Trivandrum, India, 2–5 January 2022; pp. 1–6. [\[CrossRef\]](#)
19. Kumar, P.; Jain, G.; Palwalia, D.K. Genetic algorithm based maximum power tracking in solar power generation. In Proceedings of the 2015 International Conference on Power and Advanced Control Engineering (ICPACE), Bengaluru, India, 12–14 August 2015; pp. 1–6. [\[CrossRef\]](#)
20. Lian, K.L.; Jhang, J.H.; Tian, I.S. A Maximum Power Point Tracking Method Based on Perturb-and-Observe Combined With Particle Swarm Optimization. *IEEE J. Photovolt.* **2014**, *4*, 626–633. [\[CrossRef\]](#)
21. Nugraha, D.A.; Lian, K.L.; Suwarno. A Novel MPPT Method Based on Cuckoo Search Algorithm and Golden Section Search Algorithm for Partially Shaded PV System. *Can. J. Electr. Comput. Eng.* **2019**, *42*, 173–182. [\[CrossRef\]](#)
22. Tomar, Y.; Lian, K.L. A Novel MPPT Method Based on Crow Search Algorithm Combined with Perturb & Observe for Partial Shading Conditions. In Proceedings of the 2021 IEEE 12th Energy Conversion Congress & Exposition—Asia (ECCE-Asia), Singapore, 24–27 May 2021; pp. 1475–1480. [\[CrossRef\]](#)
23. Liao, C.Y.; Subroto, R.K.; Millah, I.S.; Lian, K.L.; Huang, W.T. An Improved Bat Algorithm for More Efficient and Faster Maximum Power Point Tracking for a Photovoltaic System under Partial Shading Conditions. *IEEE Access* **2020**, *8*, 96378–96390. [\[CrossRef\]](#)
24. Abo-Khalil, A.G.; El-Sharkawy, I.I.; Radwan, A.; Memon, S. Influence of a Hybrid MPPT Technique, SA-P & O, on PV System Performance under Partial Shading Conditions. *Energies* **2023**, *16*, 577. [\[CrossRef\]](#)
25. Koh, J.S.; Tan, R.H.G.; Lim, W.H.; Tan, N.M.L. A Modified Particle Swarm Optimization for Efficient Maximum Power Point Tracking under Partial Shading Condition. *IEEE Trans. Sustain. Energy* **2023**, *14*, 1822–1834. [\[CrossRef\]](#)
26. Ishaque, K.; Salam, Z.; Amjad, M.; Mekhilef, S. An Improved Particle Swarm Optimization (PSO)-Based MPPT for PV With Reduced Steady-State Oscillation. *IEEE Trans. Power Electron.* **2012**, *27*, 3627–3638. [\[CrossRef\]](#)
27. Makhloufi, S.; Mekhilef, S. Logarithmic PSO-Based Global/Local Maximum Power Point Tracker for Partially Shaded Photovoltaic Systems. *IEEE J. Emerg. Sel. Top. Power Electron.* **2022**, *10*, 375–386. [\[CrossRef\]](#)
28. Millah, I.S.; Chang, P.C.; Teshome, D.F.; Subroto, R.K.; Lian, K.L.; Lin, J.F. An Enhanced Grey Wolf Optimization Algorithm for Photovoltaic Maximum Power Point Tracking Control under Partial Shading Conditions. *IEEE Open J. Ind. Electron. Soc.* **2022**, *3*, 392–408. [\[CrossRef\]](#)
29. Teshome, D.F.; Lee, C.H.; Lin, Y.W.; Lian, K.L. A Modified Firefly Algorithm for Photovoltaic Maximum Power Point Tracking Control under Partial Shading. *IEEE J. Emerg. Sel. Top. Power Electron.* **2017**, *5*, 661–671. [\[CrossRef\]](#)
30. Mohammed, K.K.; Mekhilef, S.; Buyamin, S. Improved Rat Swarm Optimizer Algorithm-Based MPPT under Partially Shaded Conditions and Load Variation for PV Systems. *IEEE Trans. Sustain. Energy* **2023**, *14*, 1385–1396. [\[CrossRef\]](#)
31. Mohammadi-Balani, A.; Dehghan Nayeri, M.; Azar, A.; Taghizadeh-Yazdi, M. Golden eagle optimizer: A nature-inspired metaheuristic algorithm. *Comput. Ind. Eng.* **2021**, *152*, 107050. [\[CrossRef\]](#)
32. Yao, X.; Liu, Y.; Lin, G. Evolutionary programming made faster. *IEEE Trans. Evol. Comput.* **1999**, *3*, 82–102. [\[CrossRef\]](#)
33. Farh, H.M.H.; Othman, M.F.; Eltamaly, A.M.; Al-Saud, M.S. Maximum Power Extraction from a Partially Shaded PV System Using an Interleaved Boost Converter. *Energies* **2018**, *11*, 2543. [\[CrossRef\]](#)
34. Farh, H.M.; Eltamaly, A.M.; Al-Saud, M.S. Interleaved boost converter for global maximum power extraction from the photovoltaic system under partial shading. *IET Renew. Power Gener.* **2019**, *13*, 1232–1238. [\[CrossRef\]](#)
35. Eltamaly, A.M.; Farh, H.M.H.; Al Saud, M.S. Impact of PSO Reinitialization on the Accuracy of Dynamic Global Maximum Power Detection of Variant Partially Shaded PV Systems. *Sustainability* **2019**, *11*, 2091. [\[CrossRef\]](#)
36. CSN EN 50530; Overall Efficiency of Grid Connected Photovoltaic Inverters. BSI Standards: Singapore, 2010.

Disclaimer/Publisher’s Note: The statements, opinions and data contained in all publications are solely those of the individual author(s) and contributor(s) and not of MDPI and/or the editor(s). MDPI and/or the editor(s) disclaim responsibility for any injury to people or property resulting from any ideas, methods, instructions or products referred to in the content.